Inverse parabolic quantum wells grown by molecular-beam epitaxy using digital and analog techniques

W. Q. Chen, S. M. Wang, T. G. Andersson, and J. Thordson
Department of Physics, Chalmers University of Technology, S-412 96 Göteborg, Sweden
(Received 2 June 1993)

An $Al_{0.36}Ga_{0.64}As/Al_xGa_{1-x}As$ inverse parabolic quantum-well structure was grown by molecular-beam epitaxy using both digital and analog compositional grading techniques. Photoluminescence and photocurrent measurements showed distinct exciton peaks for both types of wells. A large Stark shift was found for the digital well, in agreement with the calculations. An observed deviation for the analog well was ascribed to fluctuation in quantum-well parameters. Finally, advantages and disadvantages of the two growth techniques are discussed.

There is a recent growing interest in the electric-field dependence of semiconductor quantum-well optical properties. The most extensively studied and utilized is the quantum-confined Stark effect (QCSE) which is a shift of the exciton absorption edge to lower energy with an electric field applied to the quantum well. This effect offers tunable optical response that can be used in a number of device applications, such as high-speed optical modulators,[1] optical bistable devices,[2] and photodetectors.[3] Most studies on the QCSE have focused on square wells. These can easily be grown by molecular-beam epitaxy (MBE), only using the simple shutter on-off operation. Extension of the QCSE studies from square to nonsquare wells provides us with a freedom in the production of tailor-made and tunable electro-optic effects. A number of recent studies on nonsquare wells[4–11] revealed an enhanced Stark effect. This stimulated us to further investigate the effect of quantum-well shapes.

Atomic layer-by-layer deposition makes it possible to grow nonsquare quantum wells in two different ways. The digital technique,[12] using a variable superlattice compositional grading, has been utilized to fabricate parabolic,[12] triangular,[6,7] and compositionally graded bottom[11] wells. The analog technique,[13] providing a continuous compositional grading, was recently attempted to grow parabolic[13] and triangular[14] wells. However, there are only a few reports on the growth of very narrow wells and no comparative studies of quantum structures as a result of these two techniques. In this paper we report the fabrication of an inverse parabolic quantum well (IPQW) by MBE using either the digital or analog techniques. We also studied the quantum-confined Stark effect in them. Comparative study of the inverse parabolic quantum well with the conventional square well will be reported elsewhere.[15]

Samples having inverse parabolic quantum wells were grown in a Varian GEN II MBE system by digital and analog techniques, respectively. The structures were grown on n^+-type GaAs (100) substrates with a growth rate of 0.5 μm/h. The layer sequence consisted of a 0.1-μm Si-doped GaAs buffer layer followed by 0.1-μm $Al_{0.36}Ga_{0.64}As$, five repeats of a 130-Å parabolic-well layer separated by 250-Å $Al_{0.36}Ga_{0.64}As$ barriers, a 0.1-μm $Al_{0.36}Ga_{0.64}As$ layer, and finally 100-Å GaAs as a cladding layer. In order to mimic an ideal IPQW potential shown in Fig. 1(a), the Al composition x in the well layer was graded by the digital technique in one sample and analog-migration-enhanced epitaxy in the other, as illustrated in Figs. 1(b) and 1(c).

The digital IPQW was fabricated via a continuous growth of a variable $Al_{0.36}Ga_{0.64}As/GaAs$ superlattice with a constant period $d=10$ Å. The thickness of the GaAs layer, l_{GaAs}, centered at the middle of each period, was varied according to the following expression:

$$l_{GaAs}=d\left[\frac{x_0-x_f}{x_0}-\frac{x_i-x_f}{x_0}\frac{(2n-N-1)^2}{N^2}\right], \quad 1\le n\le N, \quad (1)$$

where x_i and x_f are the average Al composition at the edge and center of the well, respectively. The Al composition in the barrier is x_0 and N ($=13$) is the total number of periods in the superlattice.

For the growth of the analog well, it is difficult to continuously adjust the furnace temperature to get a good parabolic profile of the Al composition across just 130 Å. Instead, the total well thickness was divided into 23 periods. For each period (two monolayers), the furnace temperature of the Al source was manually set to a specific value associated with the designed Al composition. A growth interruption (<2 min) was adopted between each layer in the migration-enhanced epitaxy growth.[16]

A semitransparent Au Schottky contact was deposited on top of the GaAs layer. Photoluminescence (PL) and photocurrent (PC) measurements were made for the two samples. The quantum-well luminescence was excited by a He-Ne laser and measured by a standard lock-in technique, utilizing a SPEX 1704 monochromator and an S-1 photomultiplier detector. The PC signal was taken with the use of a halogen lamp. Both PL and PC measurements were made at 77 K. The built-in voltage was estimated to be 0.7 V for the digital well and 0.8 V for the

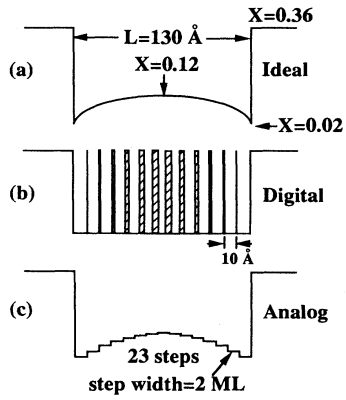

FIG. 1. (a) The ideal potential of an inverse parabolic quantum well used in the calculations. It is composed of thick $Al_{0.36}Ga_{0.64}As$ barriers and an $Al_xGa_{1-x}As$ well where the composition x varied parabolically from 0.02 at the edge to 0.12 at the center. To mimic such an ideal potential in the well region, an Al composition grading was made in two ways. In (b) is an $Al_{0.36}Ga_{0.64}As/GaAs$ variable superlattice structure having a constant period of 10 Å and (c) is an analog structure with a multiple step x variation of the $Al_xGa_{1-x}As$. The x variation for the analog well was made in 23 steps (two monolayers each) across the 130-Å well. The x value in each step was controlled by the Al source temperature.

analog one, based on the change of the PL spectra with field. The zero-field PL and PC spectra are displayed in Fig. 2. The 1e-1hh (involving the ground states) exciton resonance peak was clearly observed in both spectra and for both wells. Weak extra peaks were found as well in the PC spectra. The peak at $A2$ and $B2$ from the digital well are ascribed to the 1e-1hh and 2e-2hh transitions, respectively, since they are very close to the calculated ones indicated by arrows in the figure. For the analog well the observed peak positions are at higher energies than the calculated ones (a 15-meV deviation for the 1e-1hh transition). This error is caused by fluctuations in alloy composition and well thickness. Our calculation showed that the transition energy is more sensitively dependent on the Al composition than well thickness. For example, an error of $\Delta x_f = \pm 0.01$ (Al composition at the well center) induced ± 8.5-meV deviation of transition energy, whereas a one-monolayer error of the well thickness caused only 1-meV change in transition energy. The deviation of the alloy composition or/and well thickness could shift the transitions to higher energies but had little influence on the relative peak positions. Hence the peaks at $A1$, $B1$, and $C1$ could be ascribed to the 1e-1hh, 2e-2hh, and 2e-2lh transitions, respectively. Besides, there is an ~9-meV difference in the 1e-1hh peak energies from the PL and PC spectra for both wells. This is probably a Stokes shift[17] caused by interface roughness. It was also noted that there is a wide peak width of 1e-1hh exciton resonance for both wells. The reason for this is unclear. We believe that the dominant mechanism is an inevitable interface roughness[18] occurring within many repeated structures. Another effect could be the alloy disorder[18] which causes potential fluctuations.

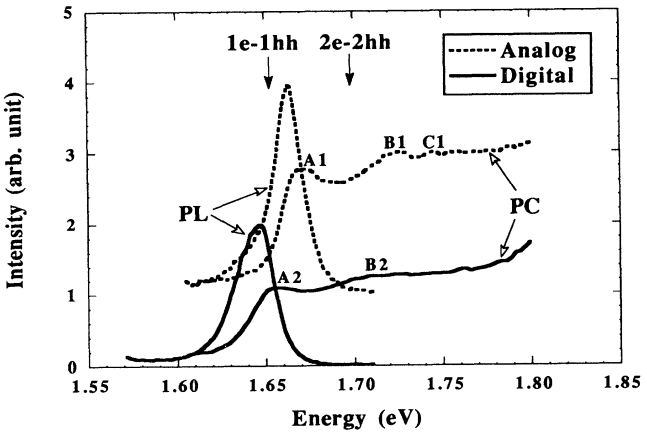

FIG. 2. Photoluminescence and photocurrent spectra measured at 77 K for the digital and analog IPQW's at zero field. The 1e-1hh exciton resonance was distinctly observed in PL spectra for both wells. The peaks in the PC spectrum for the digital well at $A2$ and $B2$ are assigned to 1e-1hh and 2e-2hh transitions, in close agreement with the calculated values indicated by arrows in the figure. Those at $A1$, $B1$, and $C1$ for the analog well could be assigned to 1e-1hh, 2e-2hh, and 2e-2lh transitions, respectively. Observed deviations from calculated values for the analog well are ascribed to fluctuations in well parameters.

Upon application of a reverse bias, the QCSE could be seen in the photoluminescence measurements. Figures 3(a) and 3(b) display representative spectra measured at different bias for the digital and analog wells, respectively. The prominent features, common for both wells, are the substantial shift to lower energy of the 1e-1hh peak, its intensity reduction, and peak width broadening with field. These characteristics are summarized for the digital and analog wells in Fig. 4 which display the energy E, the relative integrated intensity $I(F)/I(0)$, and the full width at half maximum (FWHM), respectively, of the ground-state transition as a function of applied electric field. It is obvious that the shift of the observed 1e-1hh peak is quite large for the digital well, in agreement with calculated data (the solid line). A better agreement can be obtained if the exciton binding energy and its change with electric field are considered. As a contrast, the observed 1e-1hh peak energy for the analog well is larger than the calculated one, and the deviation enlarges with field. In other words, the Stark shift is smaller than expected. This disagreement is another indication of the fluctuation in quantum-well parameters. In Fig. 4(b), we can see that the relative integrated intensity is more rapidly reduced from the digital well than the analog one: a factor of ~2. The peak reduction is mainly due to field-induced exciton polarization which leads to a decreased overlap of the 1e and 1hh wave functions. This is qualitatively reflected in the calculated squared overlap of wave functions, indicated by a solid curve in Fig. 4(b). The reason for the deviation from the calculation (ideal case) for the digital well could be complicated. There could exist defects and roughness at interfaces of the superlattice, which could influence the wave function and trap carriers, thus affect the PL intensity. The large deviation for the analog well further indicates the fluctuation in

quantum-well parameters. In Fig. 4(c), we see that the FWHM at zero field is about 25 meV for the digital well and 20 meV for the analog one, and it broadened with field for both structures but more prominently for the digital well. This broadening originates from different effects, such as carrier tunneling out of the well,[19,20] a nonuniform field, and increased sensitivity of the wave functions to the interface disorder with the field.[21]

We made calculations for the inverse parabolic quantum well by solving the effective-mass Schrödinger equation within the envelope-function framework,[22]

$$-\frac{\hbar^2}{2}\frac{d}{dz}\left[\frac{1}{m^*}\frac{d}{dz}\Psi\right]+V(z)\Psi=E\Psi\ . \tag{2}$$

For the ideal inverse parabolic potential $V(z)$ used in the calculations, the Al composition x varied according to the following expression:

$$x=\begin{cases}0.12-0.4\left[\dfrac{z}{L}\right]^2 & \text{inside the well } \left[-\dfrac{L}{2}\le z\le\dfrac{L}{2}\right]\\ 0.36 & \text{outside the well .}\end{cases} \tag{3}$$

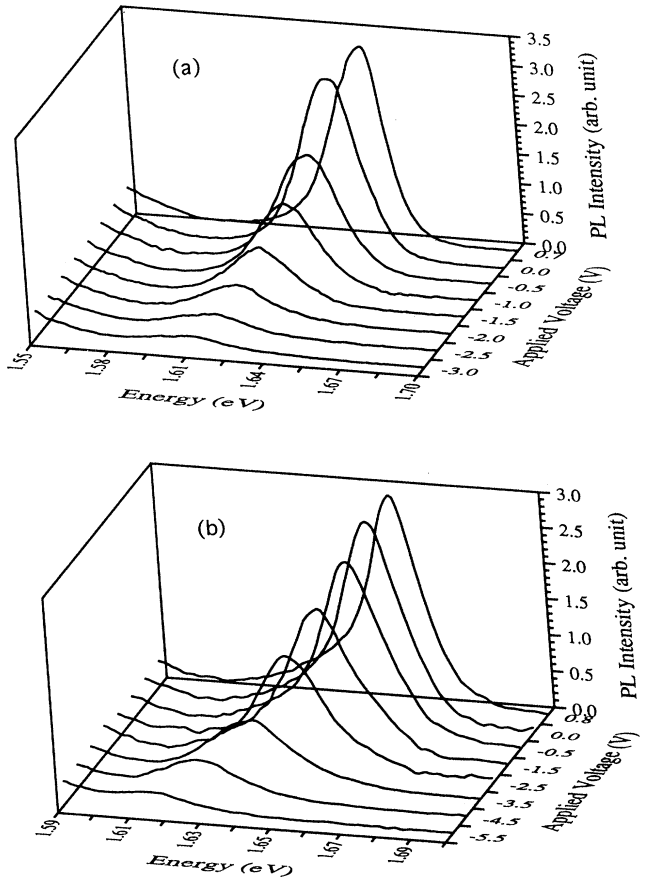

FIG. 3. Representative photoluminescence spectra measured at 77 K for (a) digital and (b) analog IPQW's at different bias. The applied voltages are indicated by the values at each curve. The built-in voltage was estimated to be 0.7 and 0.8 V for the digital and analog wells, respectively.

Here L ($=130$ Å) is the well thickness and the origin of the z axis was set at the well center. The energy gap and effective masses of $Al_xGa_{1-x}As$ were taken as

$$E_g(x)=1.508+1.247x\ \text{(eV)}\ \ \text{(at 77 K)}\ , \tag{4}$$

$$m_e^*=(0.067+0.083x)m_0\ , \tag{5}$$

$$m_{hh}^*=(0.45+0.31x)m_0\ . \tag{6}$$

The band-edge offset ratio of the conduction band Q_c was taken to be 0.6. Equation (2) was solved using a numerical method described earlier.[23]

Figures 5(a) and 5(b) display the calculated eigenenergies and wave functions of the 1e and 1hh states in the absence and presence of an electric field, respectively. For the chosen quantum-well parameters, the 1e energy level is just above the top of the parabolic barrier in the

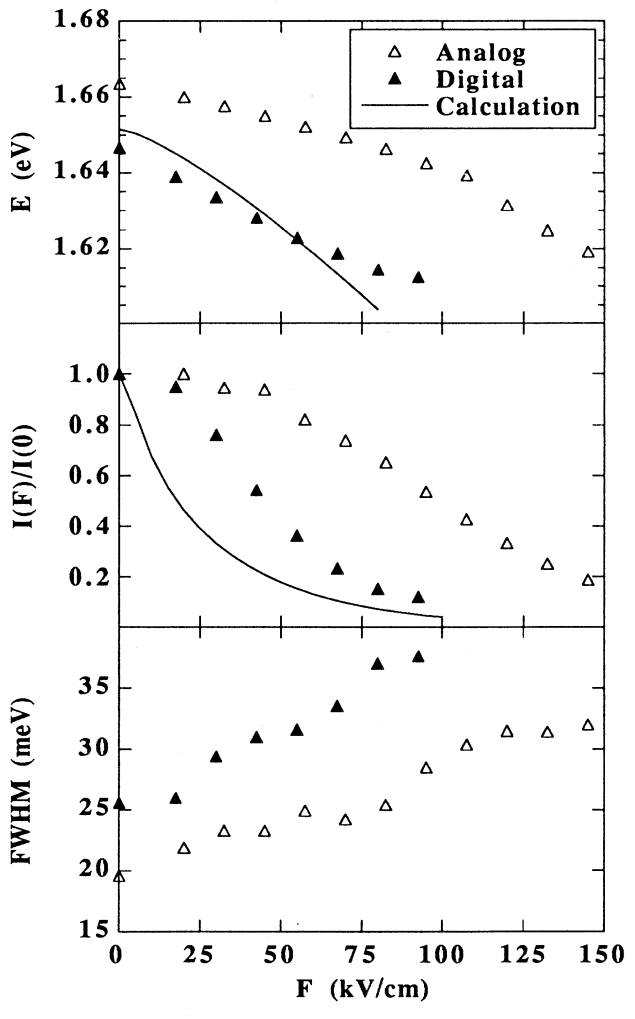

FIG. 4. (a) Transition energy, (b) relative integrated intensity, and (c) FWHM of the 1e-1hh exciton resonance as a function of applied electric field. The filled and empty triangles represent the experimental data determined from the photoluminescence measurements, as displayed in Fig. 3. The solid curves represent the calculated values.

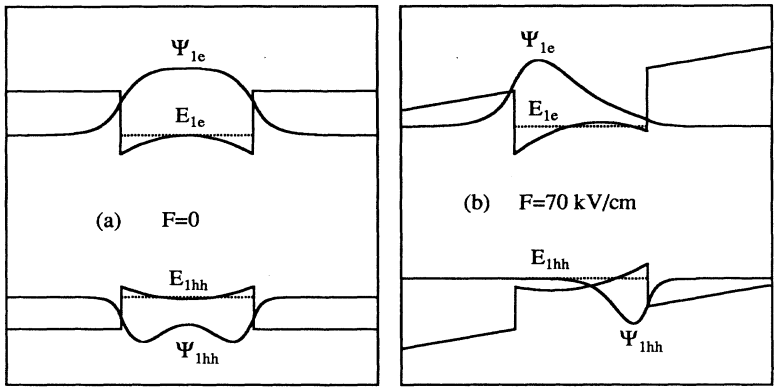

FIG. 5. The confined energies and wave functions of the electron and heavy-hole ground states for an ideal IPQW (a) without electric field and (b) at 70 kV/cm.

conduction-band well and its wave function Ψ_{1e} extends almost the whole well region (global state) in the case of zero field. As a contrast, the 1hh level is below the valence-band maximum in the middle of the well and the associated wave function Ψ_{1hh} is largely localized to the two sides (local state). A slight splitting (two meV) of the 1hh level was induced by a weak coupling of the 1hh state through the parabolic barrier. Under the applied electric field, as illustrated in Fig. 5(b), Ψ_{1e} becomes localized to one side of the well and Ψ_{1hh} to the other. Their overlap is greatly reduced, thus inducing the rapid decrease in PL intensity which was observed in Fig. 4(b) for the digital well. A quantum well with a global-to-local transition in a similar structure has been found to have a large Stark shift.[24] This was also achieved in the digital IPQW, as shown in Fig. 4(a). A comparative study, reported elsewhere,[15] indicated that the Stark shift in the digital IPQW is substantially larger than a square well having the same well thickness and depth.

The disagreement found for the analog well in Fig. 4 as compared to calculations illustrates the existence of fluctuation in Al composition and well thickness. As the period in the migration-enhanced epitaxy for the analog well is only two monolayers, it took only ~ 3.5 sec to accomplish it. This could result in a thickness error of $\pm 3.6\%$ in contrast to the shutter transition time of 0.25 sec. Besides, there are also possible errors in the Al composition from the manual setting of the Al source temperature. The calculation indicated that the deviations in quantum-well parameters not only strongly influence the energy levels but also the behavior of the quantum well under the electric field. A large Stark shift can be achieved only under the global-to-local transition condition, i.e., the 1*e* level is above the parabolic barrier in the conduction-band well while the 1hh level is well below the edge in the valence-band well. This condition may be influenced by fluctuations in well parameters. Thus we believe that the deviation found for the analog well is induced by such fluctuations.

In conclusion, comparisons between charge confinement in digital and analog inverse parabolic quantum wells were made via photoluminescence and photocurrent measurements. Distinct exciton peaks were observed in photoluminescence and photocurrent spectra for both types of wells, which indicated a good confinement of carriers in them. The largest Stark shift was found for the digital well, in agreement with our calculations. The analog well exhibited some deviations from the expected behavior, which was attributed to fluctuations in quantum-well parameters. It turns out that the digital technique is a better way to fabricate nonsquare quantum-well structures, especially for narrow ones. By this technique, one can easily and precisely control the well shape and its parameters during the MBE growth. The disadvantage is the inevitable creation of interface roughness in the superlattice, which causes exciton peak broadening. With the analog technique, on the other hand, it is not easy to control the shape and parameters for a narrow well, in spite of a narrower peak width. More interestingly, the advantage of the digital technique was also shown by a recent comparison[25] of triangular quantum wells grown by the digital and analog techniques. A better transport property was found for the digitally grown well in Hall measurements.

This work was supported by the Swedish National Science Research Council (NFR) and the Swedish National Board for Industrial and Technical Development (NUTEK).

[1]J. S. Weiner, D. A. B. Miller, D. S. Chemla, T. C. Damen, C. A. Burrus, T. H. Wood, A. C. Gossard, and W. Wiegmann, Appl. Phys. Lett. **47**, 1148 (1985).

[2]D. A. B. Miller, J. E. Henry, A. C. Gossard, and H. J. English, Appl. Phys. Lett. **49**, 821 (1986).

[3]T. H. Wood, C. A. Burrus, A. H. Gnauck, J. M. Wiesenfield, D. A. B. Miller, D. S. Chemla, and T. C. Damen, Appl. Phys. Lett. **47**, 190 (1985).

[4]W. Q. Chen and T. G. Andersson, Semicond. Sci. Technol. **7**, 828 (1992).

[5]W. Q. Chen and T. G. Andersson, Appl. Phys. Lett. **60**, 1591 (1992).

[6]K.-K. Law, R. H. Yan, A. C. Gossard, and J. L. Merz, J. Appl. Phys. **67**, 6461 (1990).

[7]P. W. Yu, D. C. Reynolds, G. D. Sanders, K. K. Bajaj, C. E. Stutz, and K. R. Evans, Phys. Rev. B **43**, 4344 (1991).

[8]T. Ishikawa, S. Nishimura, and K. Tada, Jpn. J. Appl. Phys. **29**, 1466 (1990).
[9]M. Morita, K. Goto, and T. Suzuki, Jpn. J. Appl. Phys. **29**, L1663 (1990).
[10]G. D. Sanders and K. K. Bajaj, J. Appl. Phys. **68**, 5348 (1990).
[11]T. Ishikawa and K. Tada, Jpn. J. Appl. Phys. **28**, L1982 (1989).
[12]R. C. Miller, A. C. Gossard, D. A. Kleinman, and O. Munteau, Phys. Rev. B **29**, 3740 (1984).
[13]P. F. Kopf, M. H. Herman, M. Lamont Schnoes, A. P. Perley, G. Livescu, and M. Ohring, J. Appl. Phys. **71**, 5004 (1992).
[14]S. Giugni, T. L. Tansley, F. Green, C. Shwe, and M. Gal, J. Appl. Phys. **71**, 3486 (1992).
[15]W. Q. Chen, S. M. Wang, T. G. Andersson, and J. Thordson (unpublished).
[16]S. Munnix, R. K. Bauer, D. Bimberg, J. S. Harris, Jr., R. Köhrbrück, E. C. Larkins, Ch. Maierhofer, D. E. Mars, and J. N. Miller, J. Vac. Sci. Technol. B **7**, 704 (1989).
[17]C. Delalande, M. H. Meynadier, and M. Voos, Phys. Rev. B **31**, 2497 (1985).
[18]J. Singh and K. K. Bajaj, J. Appl. Phys. **57**, 5433 (1985).
[19]L. Vina, E. E. Mendez, W. I. Wang, L. L. Chang, and L. Esaki, J. Phys. C **20**, 2803 (1987).
[20]D. A. B. Miller, D. S. Chemla, T. C. Damen, A. C. Gossard, W. Wiemann, T. H. Wood, and C. A. Burrus, Phys. Rev. B **32**, 1043 (1985).
[21]S. Hong and J. Singh, Appl. Phys. Lett. **49**, 331 (1986).
[22]P. F. Yuh and K. L. Wang, Phys. Rev. B **38**, 13 307 (1988).
[23]W. Q. Chen and T. G. Andersson, Phys. Rev. B **44**, 9068 (1991).
[24]W. Q. Chen, S. M. Wang, and T. G. Andersson, IEEE Trans. Electron Devices Lett. **14**, 286 (1993).
[25]S. M. Wang, T. G. Andersson, W. Q. Chen, U. Södervall, and J. Thordson (unpublished).